CLM-P886

CLM-P886

Some theoretical ideas relating to L-H transitions in tokamaks

F.A. Haas
A. Thyagaraja

CULHAM LABORATORY

AEA TECHNOLOGY

Some Theoretical Ideas Relating to L-H Transitions in Tokamaks

F. A. Haas and A. Thyagaraja

Abstract

We consider a set of qualitative theoretical concepts based on previously published phenomenological and turbulent transport studies and attempt to account for the observed L-H transition phenomena in divertor and limiter discharges. Possible experiments to validate or refute the above ideas are suggested and discussed.

Theory Division
Culham Laboratory

April 1990

1 Introduction

The phenomenon of L-H transition has now been very widely observed and the various features well reported. For the most up to date experimental results and their possible interpretation, the compilation of papers presented at a recent workshop at Gut Ising ("Contributions to the IAEA Technical Committee Meeting on H-Mode Physics," BURRELL 1989), should be consulted. While several different mechanisms – including the work of OHKAWA et al (1983), HINTON (1985), and BISHOP (1986) – have been suggested as possible triggers, so far none of these have proved entirely satisfactory (BURRELL et al, 1989). More recently SHAING and CRUME (1989) have proposed an interpretation based on fast ion losses and the radial electric field. This is briefly discussed later. Furthermore, apart from the work by HINTON and STAEBLER (1989), the transport aspects of the phenomenon have received little theoretical consideration. The latter workers have investigated the collisional transport for both ions and electrons in the scrape-off layer outside the separatrix. In particular, they have related the H-mode power threshold to the direction of the ion grad – B drift with respect to the X-point – a result which has received some experimental support (see for example, ASDEX and D III-D. However, as remarked by Hinton and Staebler in their paper, it is clear that classical transport alone cannot explain the observed improvement in confinement for the H-mode. Anomalous transport must play a key role.

The objective of the present paper is to consider the question of transport, both from the phenomenological and turbulence points-of-view and to attempt to give a simple, coherent, qualitative description of what might underly the phenomenon. The arguments are supported by experiment and theoretical work already available in the literature. No attempt is made to give a fully developed quantitative theory – a task well beyond us at the present time. However, our paper does suggest the form such a theory might take, as well as indicating experiments which could be undertaken to validate, or otherwise, the ideas presented here. Lastly, we shall indicate the complementary relationship of the work of Hinton and Staebler, and our own.

We begin by listing the principal properties of L – H transition which theory must interpret:

1. The L–H transition apparently involves changes in global quantities, such as average line density and β_{pol}, as well as changes at the plasma edge. It is not clear to what extent the 'centre' and 'edge' are related, and whether they could be separately modelled.

2. Although as far as edge changes are concerned, the L–H transition is a rapid process, it is to be established whether or not the process is a bifurcation.

3.The transition has a threshold that involves edge T_e or some property such as ∇T_e.

4. It is generally believed, that at transition, a transport barrier forms just inside the separatrix. Both energy and particle fluxes are reduced. In some cases the density gradient shows an enormous steepening, while the temperature gradient is only modestly affected. Edge magnetic and density fluctuations fall, and the electric field becomes more negative.

5. The H–mode is independent of heating method, and can be obtained in limiter plasmas, although confinement is poorer than is the case with separatrix operation.

6. Experiments in H,D,He, indicate (SCHISSEL et al, 1989) that energy confinement time depends significantly on the gas or gas admixture used.

7. It should be noted that in D III D, one method of exciting the H transition has been to heat the core of the discharge with ECRH. Recent experiments on JFT – 2M (HOSHINO et al 1989), however, have demonstrated that edge hreating with ECRH can trigger the H-mode, whereas core-heating is unsuccessful in this matter.

The material of the paper is presented as follows. In section 2 we briefly review two phenomenological approaches. The first part concerns the core evolution from ohmic through L-mode to H, using an anomalous resistivity approach. This shows that several global features of the ASDEX L-H transitions can be discussed in a simple unified framework without reference to edge phenomena. In the second part of this section the importance of the relative effects of inward convection and diffusion in particle transport is examined. In particular, it is shown that whatever the origin of D and V may be, in specific conditions modest changes in the ratio of V/D can result in a bifurcation-like but smooth change in global particle confinement and local density gradients. These phenomenological considerations, which are largely model independent are supplemented and strengthened by a turbulence interpretation in section 3. A shorting mechanism operating near the separatrix in poloidally diverted tokamaks is proposed to account for a change in the electrostatic potential fluctuation level in the L-H transition. A simple bifurcation model is shown to be capable of explaining qualitatively several of the the observed features of the transition in DIII-D.

2 Phenomenology

We shall divide this section into two parts. Firstly, using a complete set of fluid equations we shall describe the simulation of the slow time evolution of the global properties during L–H

transition. Secondly, using the continuity equation alone, we shall show how small changes in the transport coefficients can lead to large changes in the particle confinement time, along with the steepening of the density gradient.

(a) Slow-Time Evolution

For our immediate purpose it is sufficient to restrict ourselves to a single-fluid formulation in cylindrical geometry. For simplicity we set $T_i = T_e$ and neglect radiation in comparison with diffusive and convective losses. If required, the model can be readily upgraded to take account of these effects. The appropriate variables are $n(r,T), T_e(r,t), v_r(r,t), p(r,t), B_\theta(r,t)$ and $B_z(r,t)$, and are determined from the equations below. Thus, the continuity equation is given by

$$\frac{\partial n}{\partial t} + \frac{1}{r}\frac{\partial}{\partial r}(rnv_r) = S_p(r,t), \tag{1}$$

with the energy equation taken in the form

$$\begin{aligned}\frac{3}{2}n\left\{\frac{\partial T_e}{\partial t} + v_r\frac{\partial T_e}{\partial r}\right\} + nT_e\frac{1}{r}\frac{\partial}{\partial r}(rv_r)\\ = \frac{1}{r}\frac{\partial}{\partial r}(rn\chi_{\perp e}\frac{\partial T_e}{\partial r}) + \eta_z j_z^2 + \eta_\theta j_\theta^2 + P_{aux}(r,t)\end{aligned} \tag{2}$$

The equation of state is

$$p = 2nT_e, \tag{3}$$

with the radial momentum balance

$$\frac{\partial p}{\partial r} = \frac{1}{c}(j_\theta B_z - j_z B_\theta), \tag{4}$$

the inertial term being unimportant on the time-scales of interest.

The poloidal and toroidal components of Ampere's equations are

$$\frac{4\pi}{c}j_z = \frac{1}{r}\frac{\partial}{\partial r}(rB_\theta) \tag{5}$$

and

$$\frac{4\pi}{c}j_\theta = -\frac{\partial}{\partial r}B_z. \tag{6}$$

The poloidal and toroidal components of Ohm's law are given by

$$-\frac{v_r B_z}{c} = \eta_\theta j_\theta \tag{7}$$

$$-\frac{1}{c}\frac{\partial A_z}{\partial t} + \frac{v_r B_\theta}{c} + E_{ext}(t) = \eta_z j_z, \tag{8}$$

with **A** related to **B** in the usual way

$$B_z = \frac{1}{r}\frac{\partial}{\partial r}(rA_\theta) \tag{9}$$

$$B_\theta = -\frac{\partial A_z}{\partial r} \tag{10}$$

We note that as discussed in THYAGARAJA and HAAS (1988), the RHS' of Eqs (7) and (8) represent the elements of an **effective** resistivity tensor which is diagonal with respect to poloidal and toroidal coordinate directions. It can be shown by transforming this tensor to the local coordinates defined with respect to the magnetic field direction, that $\eta_{||} \sim \eta_z$ whilst $\eta_\perp \sim \eta_\theta$, with certain off-diagonal terms. Thus the effective resistivity tensor when viewed with respect to the local field has not only anomalous diagonal components but also off-diagonal components. We note that the **total friction** force in neoclassical theory **is** off-diagonal with respect to the local field direction since it includes contributions from the neoclassical electron viscosity tensor.

It follows from the work of BICKERTON (1978) and COPPI and SHARKY (1981) that the use of the full set of equations (continuity, ohm's law and pressure balance) with classical or neoclassical resistivity tensor inevitably leads to particle fluxes which are incompatible with experiments. We have suggested in previous work (HAAS and THYAGARAJA (1986)) a possible resolution. This requires, as indicated in the above equations, that there be both a poloidal (η_θ) and toroidal resistivity (η_z). The latter, η_z, is assumed to have the Spitzer form $[1/2(m_e/ne^2\tau_e)Z_{eff}]$, τ_e being the Braginskii collision time. The form for η_θ is now discussed below. Using Equations (4) and (7) the radial fluid velocity can be expressed as

$$v_r = -\frac{c^2\eta_\theta}{B_z^2}\frac{\partial p}{\partial r} - c\eta_\theta\frac{B_\theta j_z}{B_z^2}. \tag{11}$$

Substituting in the continuity equation, we obtain

$$\frac{\partial}{\partial t}(rn) - \frac{\partial}{\partial r}\left(rn\left[\frac{c^2\eta_\theta}{B_z^2}\frac{\partial p}{\partial r} + \frac{c^2\eta_\theta B_\theta}{4\pi B_z^2}\frac{1}{r}\frac{\partial}{\partial r}(rB_\theta)\right]\right) = S_p(r,t). \tag{12}$$

Using the Maxwell equations and Ohm's law it is straightforward to deduce that B_θ satisfies the diffusion equation

$$\frac{\partial B_\theta}{\partial t} - \frac{\partial}{\partial r}\left(B_\theta\left[\frac{c^2\eta_\theta}{B_z^2}\frac{\partial p}{\partial r} + \frac{c^2\eta_\theta B_\theta}{4\pi B_z^2}\left(1 + \frac{\eta_z}{\eta_\theta}\frac{B_z^2}{B_\theta^2}\right)\frac{1}{r}\frac{\partial}{\partial r}(rB_\theta)\right]\right) = 0. \tag{13}$$

From Eqs (12) and (13) it is immediately apparent that if the poloidal field and particle transport rates are to be comparable – as is generally believed – then it is necessary that $\eta_\theta \sim \eta_z\left(\frac{B_z}{B_\theta}\right)^2$. That is, η_θ is required to be "anomalously" large compared with the Spitzer value. For typical tokamaks η_θ/η_z will be of order 10^2, say.

Equation (11) can be alternatively written as

$$v_r = -\frac{D}{n}\frac{\partial n}{\partial r} - V \tag{14}$$

where the diffusion coefficient D and the convection velocity V are defined to be

$$D = \frac{c^2 p \eta_\theta}{B_z^2} \tag{15}$$

and

$$V = \frac{c^2 \eta_\theta p}{B_z^2}\frac{1}{T}\frac{\partial T}{\partial r} + \frac{c\eta_\theta j_z B_\theta}{B_z^2}. \tag{16}$$

Previously COPPI and SHARKY (1981) have investigated particle transport in steady - state tokamak discharges in the absence of sources. They proposed – on purely empirical grounds – that the plasma velocity should take the form of Eq(14), with, however, D of the order of the perpendicular electron thermal diffusivity $\chi_{\perp e}$. It then follows that

$$\frac{\eta_\theta}{\eta_z} \sim \frac{\chi_{\perp e} B_z^2 n e^2 \tau_e}{c^2 m_e p}, \tag{17}$$

which again indicates a value of order 10^2 under typical tokamak conditions. It should be noted that an anomalous η_θ will not significantly contribute to ohmic heating provided $\eta_\theta \leq \eta_z \left(\frac{j_z}{j_\theta}\right)^2$. In the time-dependent calculations which we have carried out, it turns out that provided η_θ is sufficiently large compared to Spitzer, the results are not sensitive to its precise value.

In a previous paper (HAAS and THYAGARAJA, 1986) we presented a detailed discussion of the numerical solution of the above set of equations. Briefly, we specified simple forms for particle and additional heating sources, along with fixed **pedestal type boundary conditions**. For η_θ we took the form $\eta_z \left(B_z/B_\theta(a)\right)^2$. Interestingly, it was found that the effective thermal diffusivity for a given experiment, could always be expressed in terms of a simple function of local β_{pol}. For example, to simulate ASDEX we found the effective thermal diffusivity could be represented as

$$\chi_{eff} = K_{\perp ohm}/n^{-1}\left(\frac{T(r,t)}{T(o,t)}\right)^{-1/2}\left\{1 + \frac{8\pi n T}{B_\theta^2(a)}1.5\right\}, \tag{18}$$

the ohmic component being empirical Gruber scaling (GRUBER, 1982), with $K_{\perp ohm} = 3 \times 10^{17} cm^{-1} s^{-1}$. In fact, with these equations and the above specified formes for η_z, η_θ and χ_{eff}, it proved possible to successfully reproduce a wide range of phenomena seen in experiments. These included ohmic and L-mode scalings, the Hugill diagram, and the density clamp phenomenon on DITE. Very significantly, however, it also proved possible to simulate several global features of the L– H transition in ASDEX. FIG. 1 shows results from an earlier experiment on ASDEX (KEILHACKER et al, 1984). FIGS. 2 and 3 compare

the simulated line averages density and average poloidal-β with experiment. Given various uncertainties, the agreement is remarkably good. Fig. 4 shows the time evolution of the central electron temperature. Unfortunately the central temperature $1/2(T_e + T_i)$ waveform is not available from experiment. However, the peak predicted theoretical value of 2.7 keV at 60 msec after the beam switch-on is in good agreement with the peak experimental value of 2.6keV (BECKER et al 1984). It should also be noted that the recent ECRH limiter H-mode experiments on JFT-2M also show the same qualitative trends as shown by the simulations described here.

In summary two aspects must be emphasised. Firstly, no attempt has been made to model the edge changes (temperature or density gradient changes, say). In these calculations fixed pedestal values are maintained throughout. Secondly, the forms of the transport coefficients are also maintained unchanged (ie through ohmic, L and H phases), although clearly, the local values must alter through the $n(r,t), T(r,t)$ dependences. Despite these assumptions, however, the time-dependencies of the line average density and poloidal -β, are well reproduced through the ohmic, L and H modes. We note that the change from L to H phase can only be achieved if the neutral beam power is above a certain threshold value, otherwise, the line average density, say, continues to fall. This threshold is essentially due to beam refuelling.

(b) Particle Confinement Time

We now use a phenomenological approach to investigate the dependence of particle confinement time on diffusivity and convection. We consider the evolution of the plasma density to be controlled by the model continuity equation

$$\frac{\partial n}{\partial t} + \frac{1}{r}\frac{\partial}{\partial r}(r\Gamma(r,t)) = S(r), \tag{19}$$

where the particle flux Γ is given by

$$\Gamma(r,t) \equiv -D(r)\frac{\partial n}{\partial r} - V(r)n, \tag{20}$$

and S is a fixed particle source. The quantities $D(r)$ and $V(r)$ are profiles of the diffusivity and inward pinch velocity, respectively; for simplicity, these have been assumed to be independent of n. Defining the plasma radius to be a, it is convenient to write D and V in the forms

$$D(r) \equiv D(a) f_D(r/a) \; and \; V(r) = V(a) f_v(r/a), \tag{21}$$

where it is usual to take the profile functions f_D and f_v as monotonically increasing. Furthermore, we specify the conditions: $f_D(1) = 1, f_v(0) = 0, f_v(1) = 1, V(a) > 0$. For the problem to be fully posed it is necessary to prescribe the boundary conditions

$$n(a,t) = 0 \; and \; \Gamma(o,t) = 0, \tag{22}$$

and the initial condition

$$n(r,o) = F_{initial}(r). \tag{23}$$

Given the above data, the initial value problem for Eq.(19) can be solved numerically in general, and in special cases, analytic solutions may be constructed in terms of known functions. The properties of $n(r,t)$ may be readily discussed in terms of two parameters, namely,

$$\tau_{diff} \equiv a^2/D(a) \tag{24}$$

and

$$C_a \equiv a\frac{V(a)}{D(a)} \tag{25}$$

Clearly τ_{diff} characterises the diffusion process, while C_a is a measure of the convective flux relative to the diffusion flux. Dimensional analysis readily shows that the particle confinement τ_p follows the "scaling law"

$$\tau_p = \tau_{diff} F(C_a). \tag{26}$$

We have discussed the method of solution of Eq (19) in an Appendix. In Fig.5 we present plots of $\log_{10}(F(C_a))$ obtained by two different methods. In Fig.6 the dependence of τ_p/τ_{diff} on the parameter C_a is illustrated. It is seen that for $C_a \sim 10$ a factor of two change in this parameter leads to an order-of-magnitude increase in τ_p/τ_{diff}.

There are three straightforward conclusions to be drawn. Firstly, that for a given convection say, a dramatic change in the particle confinement time can be induced by a modest change in the diffusivity. Secondly, this must imply, given the source, a significant steepening in the density gradient. Thirdly, it illustrates the dangers of establishing scalings without due attention being paid to boundary conditions.

(c) Discussion

We have simulated the time-evolution of a particular auxiliary heated ASDEX discharge and shown, that at least as far as the plasma properties $\bar{n}, T_e$ and β_p are concerned the experimentally observed time-dependent quantities can be reproduced in the ohmic, L and H phases, well within experimental error. The simulations are evolutionary – there being no hint of bifurcation. In this phenomenological description, the edge physics due to the divertor action played no **direct** role. The particle and energy sources were simply related to the beam

characteristics and a fixed functional form was used for the total thermal diffusivity χ_{eff}, which was the same function for ohmic, L and H phases. The anomalous particle transport in all three phases was related to an anomalous poloidal resistivity $\eta_\theta \sim \eta_{spitzer} \left(\frac{B_{tor}}{B_{pol}}\right)^2$. The existence of this theoretical description and its agreement with experimentally measured waveforms for $\bar{n}$ and β_p suggests that many of the interior global features of the L - H "transition" can be understood in purely evolutionary terms without recourse to bifurcation theory.

Turning to purely edge phenomena, the question arises as to whether the changes in edge pedestals, thresholds and gradients observed in poloidally diverted tokamaks (ASDEX, D III D) are due to bifurcation in the vicinity of the separatrix. Our pupose has been to show that while such bifurcations may indeed be possible, rather sharp changes in observed quantities like densities, temperatures and global confinement times (especially of particles), can be understood entirely in terms of smooth and fairly modest variations of local particle energy transport coefficients. This was demonstrated using a model continuity equation. In particular it was shown that the particle confinement is very strongly dependent on the nondimensional parameter $\frac{aV(a)}{D(a)}$, as shown in Fig.(6). Thus if this parameter and the profiles have suitable behaviour in the L-phase, a fairly modest increase in V relative to D can trigger a very large increase in τ_p as compared to the diffusion time-scale $a^2/D(a)$. For fixed S, this implies a rapid increase of line averaged density, edge density pedestal and density gradients. Thus considering specifically the D III D H-mode due to ECRH, S will be unchanged by the ECRH. When the threshold conditions are met, that is when the profiles of D and V are appropriate prior to the heating, modest changes of D and V can result (as shown by direct numerical simulation) in large increases of the density gradients and $\bar{n}(t)$. We are aware of course, that D and V are caused by a combination of $\mathbf{E} \times \mathbf{B}$ turbulence and neoclassical effects. The same considerations apply to the electron and ion energy equations, although it is not clear whether the inward thermal pinch velocity is comparable with the thermal diffusivity χ. Thus, if $aV_T(a) << \chi(a)$, the temperature profiles will experience a much smaller change. The energy confinement time, while increased, will not be an order of magnitude larger than in the L-phase.

3 A Turbulence Interpretation

In this section we speculate on a possible turbulence interpretation of the L-H transition in ELM-free discharges. This is based on the findings of calculations carried out in recent transport studies (THYAGARAJA and HAAS, 1989). In this work a magnetic spectrum for δB_r was constructed in terms of four free constants. In an application to TEXT these were

determined by matching the calculated particle/energy fluxes and potential fluctuations at a particular radius. Fluxes have been obtained which compare well with the 'measured' particle, electron and ion heat fluxes. The calculated radial profiles for $e\tilde{\phi}/T_{oe}$ and $\frac{\tilde{n}_e}{n_o}$ agree very well with experiment, and show the fluctuations to be significantly non-adiabatic. Examination of the calculated fluxes shows that the particle and ion heat fluxes are essentially due to $\tilde{\mathbf{E}} \times \mathbf{B}$ (electrostatic fluctuations), while in the electron heat flux the $\tilde{\mathbf{E}} \times \mathbf{B}$ and $\delta\mathbf{B}$ contributions are comparable.

For convenience, we categorize L–H, transitions according to the change in density profile. Thus, for example, certain D III–D shots show a strong steepening in the density profile, whereas ASDEX transitions and limiter produced H-modes show only modest changes in the density profile. We discuss each of these classes in turn. In the case of D III–D, for example, it is observed that the main change near the separatrix zone in the L–H transition is a marked steepening of the density profile accompanied by a sharp fall in the edge particle flux. While the edge temperatures do rise somewhat and the energy confinement time does increase by a factor of 2, no dramatic changes in the temperature profile are observed. We now speculate on a possible interpretation of these observations, which is based on the theoretical results summarised above. We suppose that the effect of the poloidal divertor with its separatrix is mainly (provided threshold conditions are met) to 'short' out the electric potential fluctuations at the plasma periphery relative to the L-mode. The effect of this is to lower the $\tilde{\mathbf{E}} \times \mathbf{B}$ turbulence at the separatrix, and hence we would expect the particle diffusivity to alter in such a way as to lead to the steepening of the density gradient and hence the characteristic top-hat profile of the D III–D H-mode. Furthermore, even in the absence of any strong reduction of the magnetic fluctuations in the H-mode, caused by the divertor action, we can deduce that the total ion thermal diffusivity must be closer to neoclassical in the H-mode than in the L-mode, leading to better ion energy confinement and increased ion temperature at the edge. This is so because the anomalous part of the total effective ion thermal diffusivity is almost entirely due to $\tilde{\mathbf{E}} \times \mathbf{B}$.

We note, that if the changes in poloidal and toroidal flows are sufficiently small, then the steepening of the density profile must lead to an increased pressure gradient, and hence an increase in the negativeness of the radial electric field.

The above model can be given a simple mathematical form which shows how the 'shorting' effect of the divertor can lead to a bifurcation-like change in the fluctuation spectra. Thus if $W(t)$ represents $\mid \tilde{\phi} \mid^2$ at the edge (separatrix), we suppose that $W(t)$ satisfies the following simple equation

$$\frac{dW}{dt} = \gamma W(t) - \delta_1 W^2(t) - \delta_2(T_{edge})W(t). \tag{27}$$

The first term on the RHS represents very crudely the production rate of turbulence. It must not be confused with linear growth rates, but simply represents the total rate at which electrostatic turbulence is created due to all causes. The quantity γ is assumed to be the same in L and H phases and is independent of T_{edge}, but may well depend on I_p, β_{pol} etc. The coefficient δ_1 is a representation of non-linear saturation, and is of the same type as γ. The quantities γ and δ can only be calculated from first principles, from a non-linear dynamical theory of plasma turbulence. The last term, $\delta_2(T_{edge})$, represents the shorting or damping effect due to parallel transport (at or in the vicinity of the separatrix) to the divertor, and is taken to be a function of the edge temperature. It is apparent from the above equation, that if the edge conditions are such that $\gamma > \delta_2$, the steady solution of the equation, which is stable, is given by

$$W = \frac{\gamma - \delta_2}{\delta_1} > 0. \tag{28}$$

If, however, δ_2 is large enough (temperature high enough) and other conditions are met (such as α large enough), the only stable solution is $W = 0$, showing that the edge turbulence is considerably reduced if $\gamma < \delta_2$ at the edge. Thus the equation exhibits the simplest form of bifurcation – not in global properties – but in the turbulence level itself. It implies, of course, through our earlier discussion, substantial and possible dramatic changes in profiles and global transport. In particular, this model suggests a mechanism for the formation of a transport "barrier" in the vicinity of the separatrix in the H-mode ($\gamma < \delta_2$). We would like to stress that although we have discussed $W(t)$ in terms of the electrostatic potential fluctuations, it is obvious that it can equally well represent other fluctuations such as density.

Since H-modes do occur with the limiter and the ASDEX type of divertor which do not lead to such sharp density profile changes as in D III–D, a secondary mechanism of improvement in edge confinement may also exist. In this case, the reduction in the $\tilde{\mathbf{E}} \times \mathbf{B}$ flux is envisaged as being due to $\frac{\tilde{n}}{n_o}$ and $\frac{e\tilde{\phi}}{T_{oe}}$ being more adiabatically related in the H–mode than in the L–mode. Such a reduction in non-adiabaticity relative to the L–mode could be due to edge heating and a lowering of edge collisionality. The effect will clearly be weaker than a reduction in the amplitudes themselves. This mechanism may require the boundary condition $\frac{\partial \tilde{\phi}}{\partial x} = 0$ at the limiter (HAAS and THYAGARAJA, 1981).

4 Discussion

We note that the present work complements the recent work of HINTON and STAEBLER (1989). Thus the decrease of electrostatic turbulence in the H-mode, leaving $\delta\mathbf{B}$ unaffected, leads to the ion thermal conductivity approaching the neoclassical (collisional) value more

closely. This indicates that the neoclassical ion thermal conduction may be more relevant to the H-mode than the L-mode. Very recently SHAING and CRUME (1989) have published a possible alternative interpretation of the L-H transition based on neoclassical effects due to poloidal rotation and ion orbit losses. They first of all calculate the ion orbit loss at the edge of the plasma using standard neoclassical theory and neglecting effects due to turbulence. They then use the poloidal momentum balance equation of the plasma and the standard neoclassical ion stress tensor to derive an equation relating poloidal ion flow to ion orbit loss flux in steady state. It is then shown that this equation gives bifurcated solutions for the poloidal plasma velocity, as the ion collisionality is varied. The two solutions imply differing radial electric fields which are claimed to correspond to those observed experimentally in D III-D. Although this interesting theory is apparently in accordance with several experimental observations, it raises a conceptual difficulty. In order to explain a transition from an L to an H-mode, the theory should explain why the turbulence effects which are known to be present in the L-mode, are absent in the bifurcation equation. Thus, although turbulence may well go down when the electric field changes in the way envisaged by SHAING et al(1988) it is clearly necessary to include the effects of turbulence in the considerations which lead to this change in the first place. The theoretical ideas which we have discussed above have interesting implications for future experiments involving L-H transitions.

(1) It is important to experimentally confirm the changes that occur in the D/V ratio as a function of radius and time during the transition, especially near the edge. Such observations would clarify the issue of whether the changes in the density profile observed during L-H transitions are due to time-dependence of particle sources or changes in transport properties.

(2) Only simultaneous measurements of $\frac{\tilde{e\phi}}{Toe}$ and $\frac{\tilde{n}}{n_0}$ as functions of position and time during the L-H transition can resolve conclusively the question whether improvements in H-mode are related to turbulent $(\tilde{\mathbf{E}} \times \mathbf{B})$ transport. In particular measurements could be used to obtain the quantities $\gamma, \delta_1, \delta_2$ occuring in Eq(35) experimentally.

(3) Since the JFT-2M and D III-D experiments together show that both edge and core-heating can, under certain conditions, result in an L-H transition, it is very important to have measurements of the mean profiles of n_e, T_e and T_i and the fluctuations, both internally and at the edge during the transition. Only such simultaneous measurements can serve to distinguish between the mechanisms for L-H transitions modelled by us in ASDEX and our present model relating to edge physics.

(4) As we have pointed out, the study of trace impurity transport during the L-H transition, if it could be carried out, can be a very useful probe of the relative importance of neoclassical and $\tilde{\mathbf{E}} \times \mathbf{B}$ fluxes. The point is that the $\tilde{\mathbf{E}} \times \mathbf{B}$ fluxes for the impurities can be expected to be the same as that of the plasma ions, whilst the impurity ion neo-classical flux can be varied at will by varying the mass and charge of the impurity.

(5) Measurement of density and potential fluctuations in L-H transition occuring with limiters can be used to test the suggestion made here that limiter H-modes are essentially due to an increase in the edge adiabaticity of the fluctuations and not to a reduction in the amplitudes of the fluctuations themselves.

5 Conclusions

The experimental data on L-H transitions represent a well-defined set of phenomena which have seen no complete explanation as yet. In the present paper we have attempted to put together a set of ideas which involve both phenomenological and turbulence based concepts. Our earlier phenomenological work can be shown to recover global features of L-H experiments. They need to be supplemented by ideas based on turbulent transport to explain specific features of L-H transitions relating to the edge regions. The issue of whether the transition is an evolutionary change or a bifurcation cannot be decided by core modelling alone. We have put forward a simple model of the edge electrostatic turbulence which exhibits a bifurcation in the presence of a separatrix. For limiter H modes the mechanism for the transition would be due to changes of adiabaticity resulting from edge heating. This model predicts (in the absence of ELMS) modest changes in the electron heat transport during L-H transition with a divertor, but substantial changes in edge particle and ion heat transport. We expect the latter to be more nearly neoclassical in the H-mode than in the L-mode due to the fall in electrostatic turbulence. Finally, we note that our qualitative predictions are made in advance of experiments proposed to be carried out in D III D with HIBP for $e\tilde{\phi}/T_{oe}$, measurements , and in TEXT with a poloidal divertor to study L-H transitions. These experiments would help to falsify or otherwise the theoretical ideas presented here.

Acknowledgement

We would like to thank Dr Gruber for his comments regarding the ratio of the ion neoclassical to the turbulent energy transport during L-H transitions in ASDEX. We are grateful to Jack Connor and Jim Hastie for constructive criticism.

References

BECKER, G et al (1984), Garching Report IPP, III/99

BICKERTON R.J. (1978), Journal Physics D: Applied Physics II, 1781.

BISHOP, C (1986) Nuclear Fusion **26**, 1063

BURRELL, K.H. (1989) "Comparison of Experiment with theory on the Basis of DIII - Results", presented at H-mode Workshop, Gut Ising

BURRELL, K.H. et al (1989), Plasma Physics and Controlled Fusion, **31**, No. 10, 1649

CARLSON, A. et al (1989), workshop: "Electrostatic Turbulence" (Cadarache)

COPPI, B and SHARKY, N (1981), Nuclear Fusion **21**, 1363

COURANT, R. and HILBERT, D (1953), Methods of Mathematical Physics, **1**, Springer, New York

GRUBER, 0 (1982), Nuclear Fusion **22**, 1349

GRUBER, O (1989), Private communication

HINTON, F.L. (1985), Nuclear Fusion **25**, 1457

HINTON F.L. and STAEBLER , G.M. (1989) Nuclear Fusion, **29**, No.3 405

HAAS, F.A. and THYAGARAJA, A. (1981), Plasma Physics, **23** 249

HAAS, F.A. and THYAGARAJA, A. (1986), Plasma Physics, **28** No.8, 1093

KEILHACKER, M et al (1984), Plasma Physics and Controlled Fusion, **26**, 49

HOSHINO, K. et al (1989), Phys. Rev. Letters **63**, No.7, 770

OHKAWA, T. et al (1983), Phys. Rev. Letters **51**, 2101

SCHISSEL et al (1989), Nuclear Fusion **29**, 185

SHAING, K.C. et al (1988), Proceedings of 12th International Conference on Plasma Physics and Controlled Nuclear Fusion Research, Nice, 1988 (IAEA, Vienna, 1989).

SHAING, K.C. and CRUME, E.C. (1989), Phys. Rev. Letters **63**, 2369

THYAGARAJA, A. and HAAS, F.A. (1989), Plasma Physics and Controlled Fusion, **31** No. 6, 965 and **31**, No. 11, 1797.

Appendix

We now discuss the method of solution of Eq.(19) in terms of the equivalent eigen-value problem as well as the use of a variational principle to determine the scaling function F.

Following standard theory (see for example, COURANT and HILBERT, 1953), the solution of Eq.(19) is given by the eigenvalue expansion

$$n(r,t) = \sum_{n=1}^{\infty} e^{-\lambda_n t} A_n \phi_n(r) \tag{A.1}$$

where

$$F_{initial}(r) = \sum_{n=1}^{\infty} A_n \phi_n(r).$$

Writing

$$\phi_n = p(r)V_n(r), \text{ where } p(r) \equiv exp\left(-\int_o^r \frac{V(r)}{D(r)} dr\right),$$

then V_n satisfies the equation

$$1/r \frac{d}{dr}(rD(r)p(r)\frac{dV_n}{dr}) = -\lambda_n p(r) V_n \tag{A.2}$$

The V_n are normalised by

$$1 = \int_o^a p(r) V_n^2 r dr$$

and satisfy the orthogonality condition

$$\delta_{mn} = \int_o^a p(r) V_n V_m r dr.$$

Note, that in terms of V_n, A_n are given by

$$A_n = \int_o^a F_{initial} V_n r dr.$$

Furthermore, as $t \to \infty$,

$$n(r,t) \simeq e^{-\lambda_1 t}\{A_1\phi_1(r) + 0(e^{-(\lambda_2-\lambda_1)t})\}$$

confinement time, τ_p, is given to a good order of approximation by

$$\tau_p \simeq 1/\lambda_1. \tag{A.3}$$

In fact, the first eigen-value, λ_1, is given by the Rayleigh–Ritz principle

$$\lambda_1 = \underset{V(r)}{Min} \frac{\int_o^a D(r)p(r)\left(\frac{dV}{dr}\right)^2 r dr}{\int_o^a p(r)V^2 dr}. \tag{A.4}$$

where the minimum is taken over real, continuously differentiable functions, such that

$$\frac{dV}{dr} = o, r = o; V = o, r = a.$$

If we are interested in investigating $F(C_a)$, and not in $n(r,t)$, we do not need to solve Eq.(19) or the eigenvalue problem, Eq. (A2). We simply take a suitable trial function $V(r)$ and calculate λ_1, approximately by calculationg the Rayleigh-quotient.

For simplicity, we take $f_D = 1$ and $f_v \equiv r/a$. Setting $r/a = x$, then

$$\lambda_1 \tau_{diff} = \overset{Min}{V(x)} \left\{ \frac{\int_o^1 e^{-1/2 C_a x^2} \left(\frac{dV}{dx}\right)^2 x dx}{\int_o^1 e^{-1/2 C_a x^2} V^2 x dx} \right\}. \tag{A.5}$$

If we now consider the trial function

$$V \equiv \frac{2}{C_a} \left(1 - exp(\frac{C_a}{2}(x^2 - 1))\right), \tag{A.6}$$

then we find

$$\frac{\tau_p}{\tau_{diff}} = R^{-1}(C_a/2) \tag{A.7}$$

where

$$R(y) \equiv 4ye^{-2y} \frac{\{(y-1)e^y + 1\}}{\{1 - 2ye^{-y} - e^{-2y}\}}. \tag{A.8}$$

For large C_a

$$R^{-1}(\frac{C_a}{2}) \simeq \frac{1}{C_a^2} exp(\frac{C_a}{2}). \tag{A.9}$$

In Fig 5, we have plotted the points obtained by fine-grid numerical solution of Eq.(19) and the curve given by Eq.(A8) for $\log_{10}(F(C_a))$. We observe that the agreement is very good. Fig 6 shows the dependence of τ_p/τ_{diff} as a function of C_a. This shows the very sensitive dependence on C_a. Thus in changing from $C_a = 7.0$ to 14.0 (a factor of 2.0), τ_p/τ_{diff} has increased by an order of magnitude. Choosing other simple forms for $f_D(r/a)$ and $f_v(r/a)$, it is found that the scaling function F does not depend sensitively on the precise choices, but only on the parameter C_a.

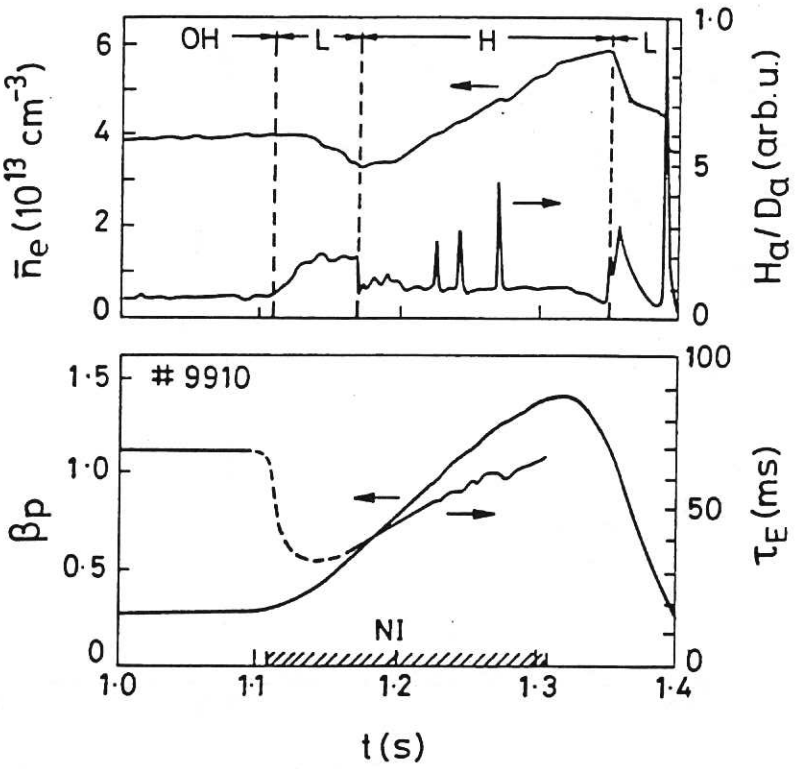

Fig. 1. Variation in ASDEX of line average electron density, $\bar{n}_e$, divertor H_α/D_α emission, $\beta_{p\perp}$ from the diamagnetic loop, and energy confinement time τ_E during neutral injection (NI) (hatched time interval), for the different confinement regions L and H (Keilhacker et al., 1984).

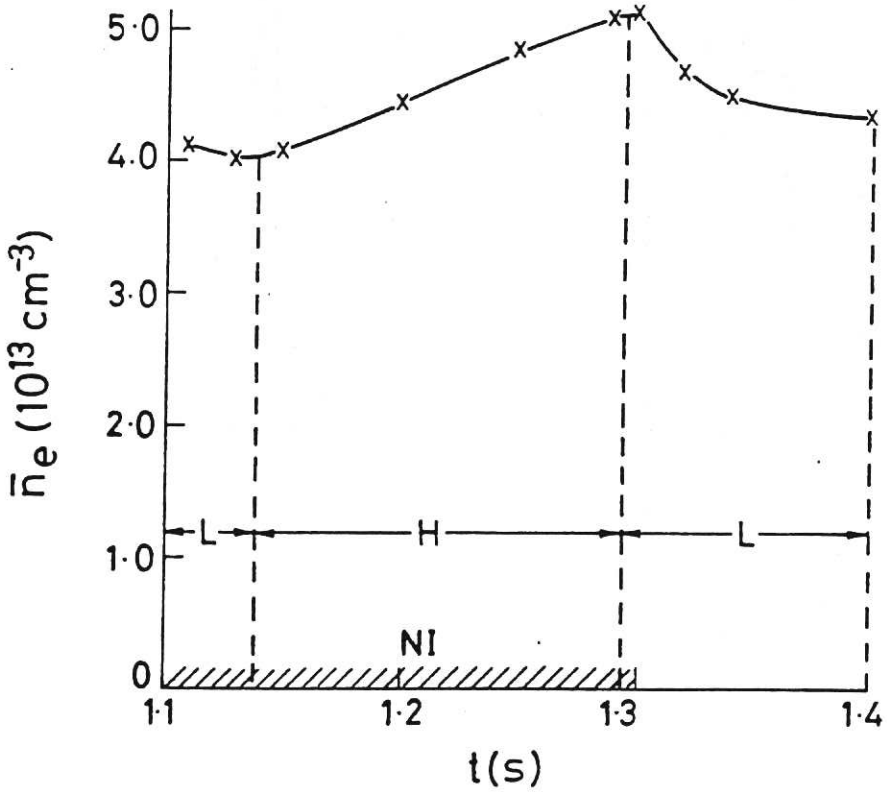

Fig. 2. Calculated time-dependence of line-averaged density in ASDEX during the neutral injection phase ($1.1 < t < 1.4s$).

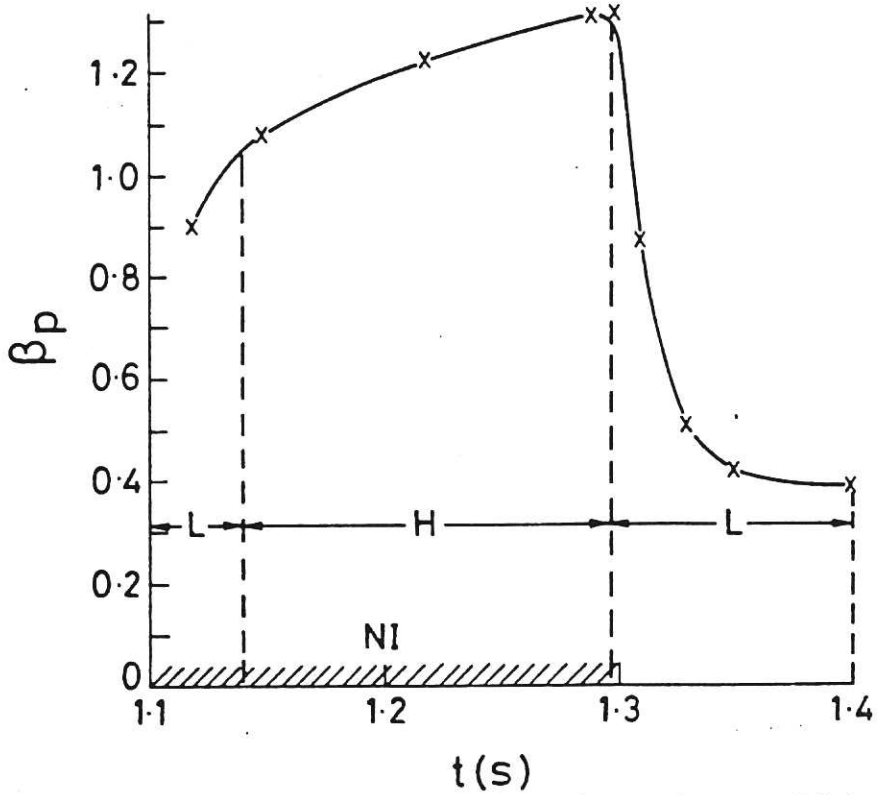

Fig. 3. Calculated time-dependence of β_p in ASDEX during the neutral injection phase ($1.1 < t < 1.4s$).

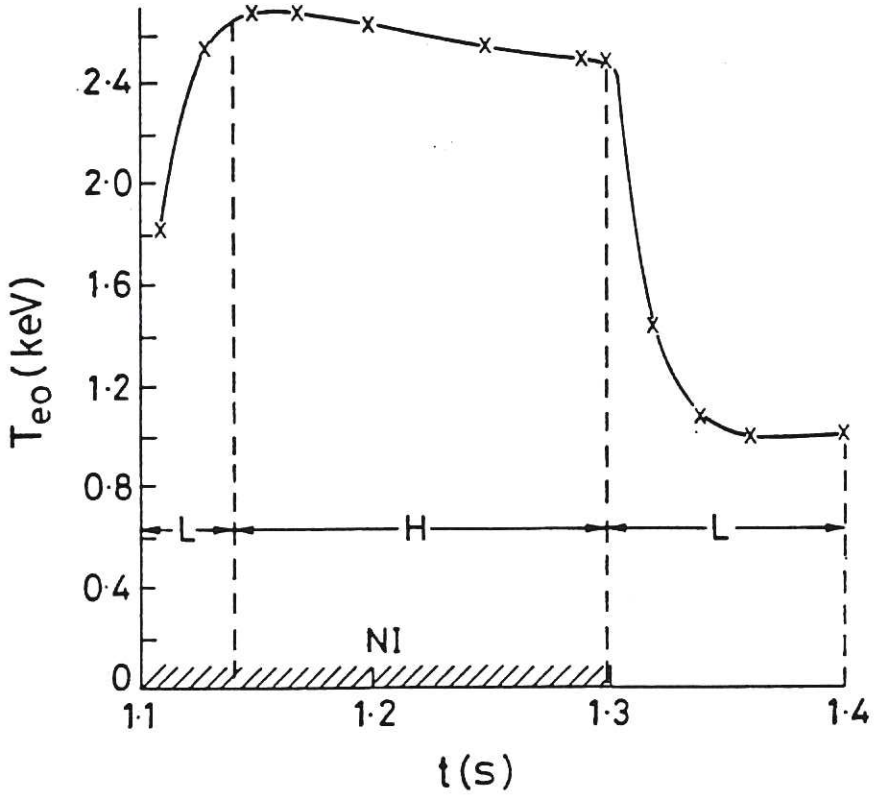

Fig. 4. Calculated time-dependence of central election temperature in ASDEX during the neutral injection phase ($1.1 < t < 1.4s$)

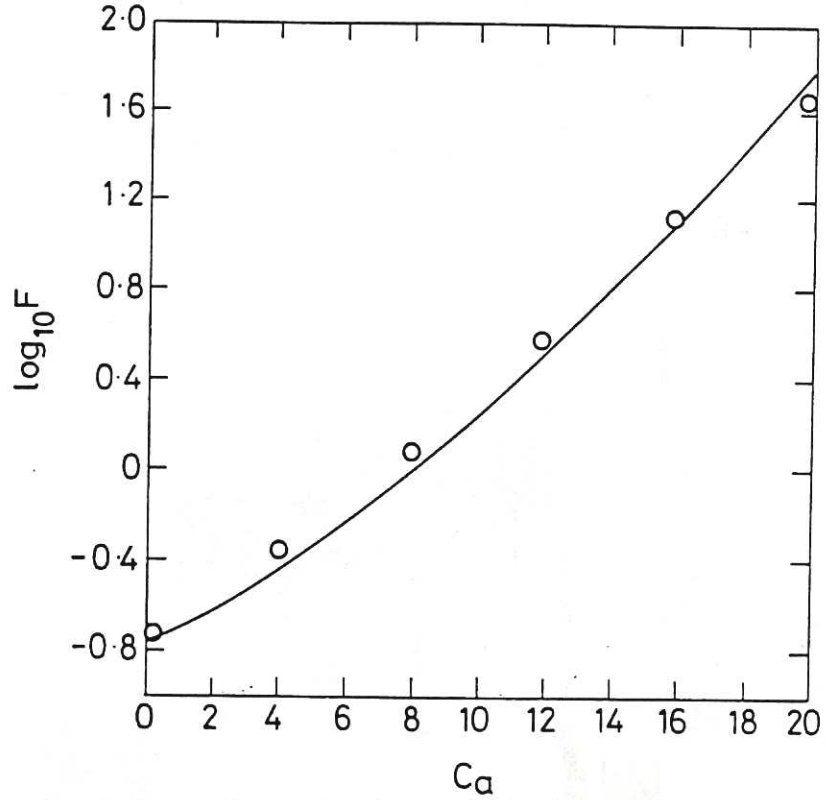

Fig. 5. comparison between the results of numerical solutions of Eq(19) (shown by open circles) and the variational formula Eq.(33)(solid curve). $Log_{10}(\tau_p/\tau_{diff})$ is plotted against C_a.

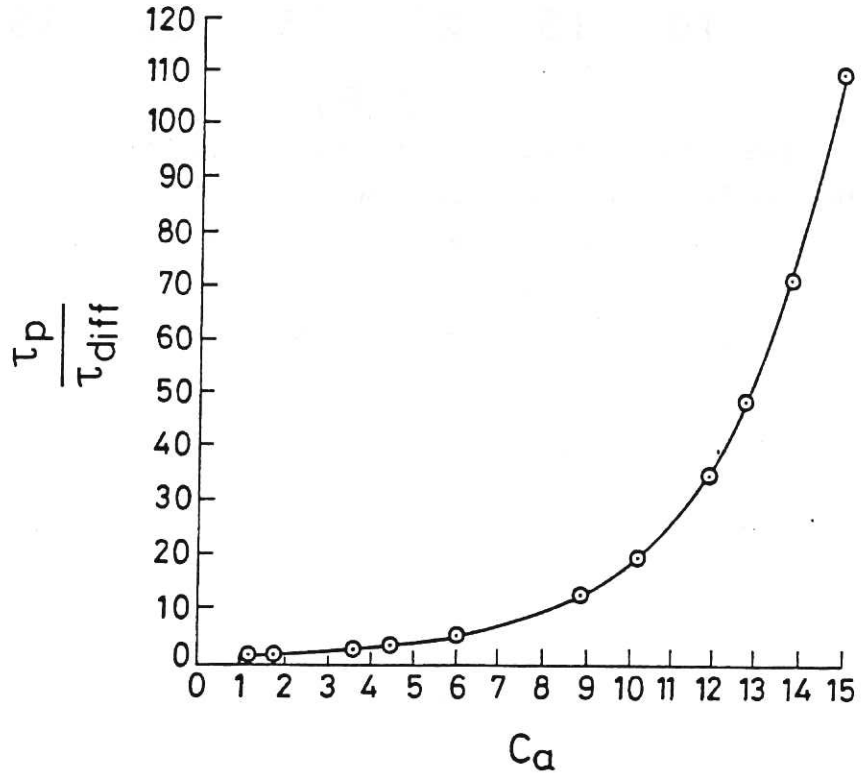

Fig. 6. Calculated variation of τ_p/τ_{diff} as a function of C_a for the specific choice $f_D \equiv 1, f_v \equiv r/a$.

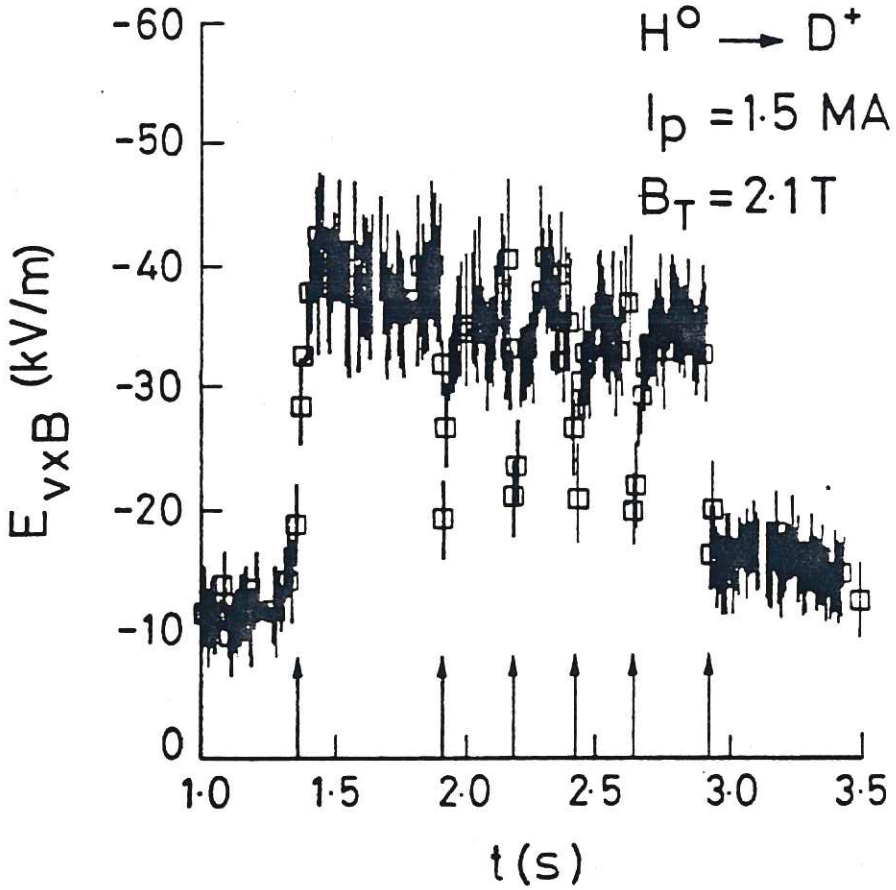

Fig. 7. Contribution to the edge radial electric field from plasma rotation as a function of time across the L to H transition. The first arrow on the X-axis indicates the time of the L to H transition. The next four arrows show when ELMS occur. The final arrow indicates the H to L transition. Notice that the electric field returns almost to its L-mode value during an ELM event. Time resolution of the spectroscopic system is 10 ms for these data.